Influencing parameters of mechanochemical intercalation of kaolinite with urea

M.-S. Yacoub Elhadj, F. Xavier Perrin

Influencing parameters of mechanochemical intercalation of kaolinite with urea

M-S.Yacoub Elhadj [a], F.Xavier Perrin [a,*]

[a] *Laboratoire Matériaux Polymères Interfaces Environnement Marin (MAPIEM EA 4323), Université de Toulon CS 60584 - 83041 TOULON CEDEX 9 – France*

* *Corresponding author.*

E-mail address: perrin@univ-tln.fr (FX Perrin)

Keywords: Kaolinite; Urea; Intercalation; Exfoliation; Mechanochemical method

ABSTRACT

Kaolinite-urea intercalates were prepared by dry grinding kaolin KGa-1b with urea using a laboratory-scale planetary ball mill. The effect of milling conditions on the intercalation process was investigated over a wide range of urea content (25 m% - 80 m%) and milling times (up to 2 h). The purification of the complex obtained was carried out by repeated washings with isopropanol in order to remove the excess (non-intercalated) urea. For that purpose, the proportion of intercalated urea and non-intercalated urea crystals was quantified after each washing step by combining differential scanning calorimetry (DSC) and thermogravimetric analysis (TGA) results obtained simultaneously. The optimal conditions of the intercalation were realized at a 66 m% urea loading for which a relatively low-defect complex structure was obtained in a short milling time. One drawback with the use of a high urea content (> 25 m%) during grinding was the presence of a large proportion of excess urea crystals in the as ground sample. This required repeated washing with isopropanol to purify the complex. Furthermore, the results revealed that washing with water the kaolinite-urea intercalates led to the formation of 0.84 nm kaolin hydrates and that exfoliation/delamination of kaolinite was more efficient when a high concentration of urea was used in the milling process.

1. Introduction

Kaolinite is a 1:1 type clay mineral built from stacked layers of tetrahedral silica sheet and octahedral Gibbsite-like sheet. The individual layers are firmly held together by hydrogen bonds. Mainly, there are two ways to intercalate urea into kaolinite layers. The first way is by the displacement of pre-intercalate molecules such as hydrazine (Ledoux and White, 1966) or DMSO (Liu et al., 2014). The second way is direct intercalation of urea into the interlayer space of pristine kaolinite, by aqueous suspension (Frost et al., 2000; Gardolinski and Lagaly, 2005a; Seifi et al., 2016), mechanochemical (Yan et al., 2005; Letaief et al., 2006a; Makó et al., 2009, 2013), and homogenization (Makó et al., 2015, 2019) methods. In the aqueous suspension method, kaolinite is mixed with a concentrated aqueous solution of urea at 25-110°C for 2-8 days, followed by centrifugation to recover the kaolinite-urea (Kaol-U) complex (Frost et al., 1997b; Gardolinski and Lagaly, 2005a; Zhang et al., 2017; Cheng et al., 2018). The mechanochemical method is based on the manual or mechanical co-grinding of urea and kaolinite with or without the presence of a small amount of water (Tsunematsu and Tateyama, 1999; Valášková et al., 2007; Makó et al., 2009; Horváth et al., 2010). A considerable number of studies reported on the effect of grinding and milling time on the structure of kaolinite (Aglietti et al., 1986a; Gonzalez Garcia et al., 1991; Sánchez-Soto et al., 2000; Frost et al., 2001a, 2001b, 2004; Franco et al., 2004; Valášková et al., 2007, 2011; Pardo et al., 2009; Vdović et al., 2010; Hamzaoui et al., 2015; Ondruška et al., 2018). Frost et al. (2004) found that the delamination of kaolinite surfaces taking place for short milling times (< 30 min to 2 h) was followed by reaggregation of the ground crystals. During dry milling, surface hydroxyls of the kaolinite were lost and replaced with water molecules coordinated to the new surface active sites (Frost et al., 2001a, 2004). In another study, Sánchez-Soto et al. (Sánchez-Soto et al., 2000) showed that grinding Georgia kaolin

produced a strong structural alteration, mainly along the c axis, resulting in disorder and total degradation of the crystal structure of the kaolinite and the formation of an amorphous product. As with the grinding of kaolin, the co-grinding of kaolin and urea resulted in structural disorders and a reduction in particle size (Makó et al., 2013). Structural disorders induced by milling can make it difficult to incorporate other organic molecules by the direct displacement method. In the homogenization method, which has been reported more recently, kaolinite is mixed with urea in an agate mortar with a small amount of distilled water and the mixture is aged in a closed or opened sample holder (Makó et al., 2015, 2016, 2017). The amount of urea used in the mechanochemical and homogenization methods was an order of magnitude less than in the suspension aqueous method. The homogenization method advantageously makes it possible to obtain a more ordered Kaol-U complex compared to mechanochemical method, but still, we are not aware of any study reporting complete intercalation of urea through this method. The optimal conditions for the preparation of the Kaol-U complex by the homogenization method were as follows: 55 m% kaolinite content, 0.7 mass fraction of urea, and aging in an open sample holder at 80°C for 24 h (Makó et al., 2019). Under these conditions, there was still about 15% kaolinite not intercalated by urea. In view of the current research status of Kaol-U intercalates, the preparation methods still need to be improved to be simple, fast, and cost-effective. In this work, ball milling in dry conditions low-defect kaolinite with urea was further explored by investigating the effect of milling conditions (milling times and urea-to-kaolin mass ratio) on the intercalation process. 10 to 40 m% urea loadings are usually used for the preparation of Kaol-U intercalates by co-grinding kaolin with solid urea (Tsunematsu and Tateyama, 1999; Letaief and Detellier, 2009; Rutkai et al., 2009). Higher urea loadings (> 40 m%) for which only a few studies are reported so far (Letaief et al., 2006a) were also tested for comparison.

The weakening of the interlayer hydrogen bonds caused by the intercalation of urea may facilitate the delamination/exfoliation of kaolinite after a subsequent treatment of the Kaol-U complex (Tsunematsu and Tateyama, 1999; Valášková et al., 2011). Therefore, the structural characteristics of kaolinite after washing the Kaol-U intercalates with water were also investigated in this paper. Another scientific problem addressed in this paper concerns the removal of excess urea (not intercalated). This purification step is important from different aspects: excess urea may decrease the efficiency of the displacement method when the Kaol-U complex is used as a pre-intercalate. On the other hand, the excess urea can lead to a significant burst release of urea in the environment which can be harmful when the intended application requires a controlled release of urea, for example for the preparation of urea controlled-release fertilizers. A further point to consider is that the washing can be accompanied by a partial deintercalation of urea, hence the need to control this purification step. To our knowledge, this problem of purification by the washing of the Kaol-U complex has not been investigated so far.

2. Experimental details

2.1. Intercalation of kaolinite with urea.

The kaolin used in this study was low defect kaolinite (KGa-1b; Georgia) from the *Source* Clays *Repository* of the *Clay Mineral Society* (CMS) with a Hinckley index (HI) of around 1.09 (Hinckley, 1962). The chemical composition of the kaolin in m% of the various oxides is : SiO_2, 44.2; Al_2O_3, 39.7; TiO_2, 1.39; Fe_2O_3, 0.13; FeO, 0.08; MnO, 0.002; MgO, 0.03; Na_2O, 0.013; K_2O, 0.05; F, 0.013; P_2O_5, 0.034 (https://www.clays.org/sourceclays_data/). The dehydroxylation mass loss of KGa-1b is 13.47% (theoretical mass loss 13.95%) indicating that KGa-1b contains 96 m% kaolinite with minor phases such as quartz, anatase, and mica (Pruett and Webb, 1993). All the particles of the original sample were passed through a 635-

mesh sieve that means kaolin particles are less than 20 µm. KGa-1b was mixed with 25, 50, 66, and 80 m% of urea (Fisher, >99%), and the mixtures (15 g) were ground for different times (5 min to 2 h) with a planetary ball mill (PM100; Retsch corporation) in a 125 cm^3 agate jar with 30 agate balls (10 mm diameter). The applied rotation speed was 400 rpm and the direction of rotation was reversed every 10 min to avoid any agglomeration with a 1 min break to prevent the powder from reaching too high temperatures. For isopropanol washing, the as-ground mixture (2g) was suspended in 15 ml isopropanol with gentle shaking for 30 s before applying vacuum to rapidly filter the dispersion. Afterwards, the product was dried at 40°C for 48 h. The total removal of urea was carried out by vigorously shaking a suspension of the as-ground mixture (1 g) in 100 ml water for 24 h at room temperature. The operation was repeated two times and then, the solid was separated by centrifugation (3000 rpm for 10 min), resuspended in 100 ml water and shaken for 1 h in an ultrasonic bath. The resulting suspension was centrifuged (3000 rpm for 10 min) to isolate the solid that was dried at 60°C for 24 h. For comparison, a KGa-1b sample was also prepared following the same treatments as Kaol-U intercalated samples.

2.2. Experimental methods

Powder X-ray diffraction (XRD) analyses were implemented on a Siemens D5000 type diffractometer equipped with a vertical goniometer and diffracted beam monochromator. The radiation applied was Cu Kα (λ = 0.1541 nm) generated at 40 kV and 40 mA. The samples were measured in step scan mode with 0.04° step size and 4 s step scan. The degree of intercalation α was calculated using the integral intensity of the (001) reflections of the unexpanded kaolinite, I_0 and the intercalation compound, I (Gardolinski and Lagaly, 2005b): $\alpha = 100.I/(I+I_0)$. Simultaneous DSC/TGA was performed using a TA Instruments SDT600 heating rate under continuous nitrogen purge of 100 mL/min. The

samples (ca. 10 mg) were typically equilibrated at 30°C and ramped to 800°C at a rate of 10°C/min and data analysis was performed using Universal Analysis 2000 software package. The Fourier transform infrared (FTIR) spectra were recorded on a FTIR spectrometer Nexus, (ThermoNicolet) equipped with an attenuated total reflectance diamond crystal unit (Thermo Scientific Smart iTR). 32 scans were obtained at a resolution of 4 cm^{-1} and over a spectral range of 600-4000 cm^{-1}. Scanning electron microscopy (SEM) images were recorded with a Zeiss Supra 40 VP Field Emission Scanning Electron Microscope in the secondary electron mode and at an accelerating voltage of 3 kV. The samples were mounted on aluminum stubs with a double-sided adhesive carbon disk and coated with a thin layer of gold to prevent charging of the surface.

3. Results and discussion

3.1. Effect of milling conditions on the characteristics of Kaol-U intercalate

A urea loading of 25 m% was selected because it corresponds to commonly used loading conditions. Ball milling was more rarely carried out with > 40 m% urea loadings. Consequently, it seemed interesting to study samples with urea loadings of 50 m%, 66 m%, and 80 m%, in addition to the 25 m% urea loading sample. When kaolin was ground with 80 m% urea, the powder stuck to the jar walls and the balls even after short milling times. This sample was therefore not further studied. In agreement with previous studies (Letaief et al., 2006b; Makó et al., 2009, 2013, 2017, 2019), the intercalation of urea into kaolinite resulted in a displacement of the (001) reflection to a lower angle (Fig. 1 and Fig. S1). For the raw kaolinite, the d-value was 0.71 nm, but when it was intercalated by urea, the d-value was shifted to 1.07 nm. The degree of intercalation increased significantly with the grinding time. The kaolin co-ground 1/4 h with 66 m% solid urea led to 94% intercalation while the rate of intercalation was only 47% when kaolin was co-ground with 25 m% solid urea. 1 h of co-

grinding kaolin with 66 m% urea led to almost 100% intercalation while 2 h of grinding was necessary to obtain a high degree of intercalation (94%) with 25 m% urea. The efficiency of urea intercalation with the 50 m% urea loading sample was intermediate (87 and 96% intercalation were calculated after 1/4 h and 1 h grinding time, respectively) between that of the sample loaded with 25 m% urea and that of the sample loaded with 66 m% urea. The XRD results showed that an excess of urea increases the ability of the kaolinite layers to be expanded by urea. High degrees of urea intercalation by mechanochemical treatment were reported in the literature for grinding times greater than 1 hour (Makó et al., 2013). Here, 1/4 h of co-grinding was sufficient to achieve almost complete intercalation when kaolin is co-ground with a small excess of urea (66 m% urea). This is the most interesting result of the present study. Moreover, the relatively sharp profile of the (001) reflection at 1.07 nm after 1/4 h co-grinding showed that the Kaol-U complex was well-ordered with a large crystallite size along the *c* axis. It is noted that the influence of the urea content on the degree of intercalation by the mechanochemical method appears opposite to that observed by the homogenization method which led to an increasing degree of intercalation with the level of kaolinite up to 70 m% of kaolinite (Makó et al., 2019). A significant broadening of the 1.07 nm reflection was observed when grinding time increased which can be related to the increase of the mean lattice strain and/or to the reduction of the crystallite size during mechanochemical process (Makó et al., 2009). The full width at half-maximum (FWHM) value of the 1.07 nm reflection was slightly broader for the intercalate prepared with 25 m% urea compared to those prepared with 66 m% urea. This result suggests that co-grinding kaolinite with an excess of urea led to the formation of greater crystallite size of Kaol-U complexes along the *c* axis. For the rest of the study, we studied more specifically two urea loadings, 25 m% (the most common loading) and 66 m% which gave the higher efficiency of

169 intercalation. The morphology of the untreated kaolin and the different treated kaolin
170 samples was observed by SEM (Fig. 2). Micrograph of the untreated kaolin revealed the
171 typical booklet morphology of kaolinite with many stacked euhedral pseudohexagonal
172 platelets with a lateral size mostly less than 4 μm. After 1 h grinding without urea, kaolinite
173 did not exhibit the booklet morphology and there was less stacking of the kaolinite particles,
174 but the hexagonal shape of the particles was largely preserved (Fig. 2, b). Fig. 2f showed XRD
175 patterns of starting kaolin before and after one hour of dry grinding. The HI value of raw
176 kaolinite was 1.09 which indicated that KGa-1b belongs to the category of ordered kaolinite.
177 After 1 h grinding, a significant loss in the definition of reflections occurring between 19 and
178 24° (2θ) was observed, suggesting that grinding results in some structural disorder. At the
179 same time, the width and intensity of the (001) reflection remained almost unchanged while
180 the d-value slightly increased from 0.713 nm to 0.718 nm. Overall, XRD results indicated that
181 the applied milling regime resulted in small structural changes for kaolinite, which agrees
182 with SEM observations. These results can be compared with those obtained recently by
183 Ondruška et al. (2018). These authors have indeed used the same type of planetary mill.
184 Milling balls made of a high-density material lead to high kinetic energy provided in the
185 collision (Štefanić et al., 2007). Despite the use of heavier corundum balls (ρ = 3.8 g/cm^3)
186 instead of agate balls (ρ = 2.4 g/cm^3), the XRD reflections of kaolinite after 1 h grinding time
187 also showed little amorphization of kaolinite (Ondruška et al., 2018). After 1/4 h grinding
188 kaolin with 66 m% urea still showed many stacks of euhedral pseudohexagonal platelets
189 with no delamination (Fig. 2, c). The SEM observations fit well with the XRD results which
190 suggested the formation of well-ordered Kaol-U intercalates after 1/4 h co-grinding. Co-
191 grinding kaolin with solid urea for longer grinding times (1 or 2 h) led to more significant
192 changes in morphology (Fig. 2, d, and e). After 1 h grinding kaolin with 66 m% urea, a few

plates still showed developed euhedral edges but most of them were somewhat irregular. It was seen that 2 h grinding kaolin with 25 m% urea led to an even greater modification of the morphology of the original kaolinite with the formation of shapeless agglomerates consisting of partially fused nanometer-sized particles giving them an apparent rugged surface. The derivative thermogravimetric (DTG) curves in Fig. 3 showed the complex nature of the decomposition of the Kaol-U samples. The first mass loss, below 125°C, was assigned to the removal of adsorbed/coordinated water. The amount of water loss increased as the grinding time increased, following other reported works (Gonzalez Garcia et al., 1991; Sánchez-Soto et al., 2000; Frost et al., 2001b; Hamzaoui et al., 2015). The increase in the amount of water loss in TGA is attributed to “gel water” formed by mechanochemical dehydroxylation from the structural hydroxyl groups of kaolinite (Makó et al., 2009). The second mass loss step, between 135 and 400°C indicated the existence of a complex multistep mechanism which is related to the loss of urea (non-intercalated and intercalated) and the residue of coordinated water (Kristóf et al., 1998). The decomposition pattern of urea drastically changed with grinding time (and thus, an increasing amount of intercalated urea) which suggests that the intercalated urea does not follow the same decomposition pathway as the adsorbed (external) urea. Notably, after 2 h grinding and near-complete intercalation of urea (from XRD results), no mass loss was observed between 250 and 350°C, as discussed below. The third mass loss step, between 400 and 800°C, is due to the dehydroxylation of kaolinite with the formation of meta-kaolinite (Miller and Oulton, 1970; Aglietti et al., 1986a; Frost et al., 1997a, 1997b, 2000, 2003; Horváth et al., 2003; Makó et al., 2009, 2013). The dehydroxylation of kaolinite took place at 514°C for original kaolinite and at 500, 487 and 482°C for the kaolin milled with 25 m% urea for 1/4, 1, and 2 h, respectively. Thus, the

dehydroxylation peak temperature of kaolinite shifted to a lower temperature as the grinding time increased. This feature will be further discussed later in this paper.

3.2. Isopropanol washes for excess urea removal

The objective of the washing step with isopropanol was to eliminate the excess urea crystals. The solubility of urea in isopropanol is lower than in other alcohols (such as methanol or ethanol) which should allow better control of the washing process by decreasing the risk of removal of interlayer urea during washing (House and House, 2017). Fig. 4 showed the thermogravimetric analyses of the kaolin ground with 66 m% solid urea for 1 h before and after three and seven successive washing steps with isopropanol. Fig. 4 also displayed the TGA curve of urea. The thermal decomposition of urea under an N_2 atmosphere is a very complex process. Based on the study by Schaber et al. (2004), the mass loss below 190°C was principally associated with urea decomposition, first resulting in the evolution of NH_3 (g) and HNCO (g). From 160°C, HNCO (g) reacts with intact urea to produce biuret and from 175°C, small amounts of cyanuric acid(s) and ammelide(s) commence to be produced from common reactants, biuret, and HNCO. Between 190 and 250°C, urea continues and biuret begins to decompose to produce large quantities of cyanuric acid and ammelide. Ammeline begins to be formed in this temperature range. The mass loss above 250°C was related to the sublimation and eventual decomposition of cyanuric acid, ammeline, and ammelide. TGA curves in Fig. 4 showed a progressive decrease in mass losses above 250°C during successive washes, *i.e.* when excess external urea is eliminated. This suggests that decomposition of intercalated urea takes place by a reaction process different in terms of total product distribution and/or intermediates observed than urea. As no mass loss was observed above 250°C when external urea was totally eliminated, intercalated urea most likely degrades without producing appreciable amounts of cyanuric acid, ammeline, and ammelide.

Simultaneous DSC/TGA can be used to study the morphological state of urea in the samples obtained after co-grinding kaolin with solid urea. The DSC curves of the ground samples before and after isopropanol washes are shown in Fig. 5. The endothermic peak at 135°C in the DSC curves was attributed to the melting of urea crystallites. In the DSC curves of the ground samples, it is clearly seen that the amount of crystalline urea decreased with isopropanol washings. It is reasonable to suppose that the intercalated urea is in an amorphous state because the interlayer space is not large enough for urea crystallization. The area of the endothermic peak at 135°C is thus directly proportional to the amount of external surface urea crystallites. The above results showed that external urea was progressively removed after isopropanol washing. From the DSC curves of the kaolin ground for 2 h with 25 m% urea, it is seen that total elimination of external urea required three successive washes with isopropanol. On the other hand, DSC curves of the kaolin ground for 1 h with 66 m% urea still showed an endothermic melting peak of urea even after seven successive washing steps, indicating that much more washings are needed for the total elimination of external urea when large amounts of urea were used in the kaolin-urea mixture. The following method can be implemented to give a more quantitative description of the type and amount of urea in the kaolin-urea samples. The mass loss in TGA between 135 and 400°C was used to determine the total urea content. Based on this method, the amount of urea in the as ground kaolin-urea samples (corrected from the physisorbed water loss below 135°C) was 27 m% for the kaolin co-ground with 25 m% urea and 67 m% for the kaolin co-ground with 66 m% urea, which is close to the expected values. The slight differences between the expected and calculated values are likely due to a small contribution from the coordinated water produced during the mechanochemical degradation to the loss of mass measured between 135 and 400°C. The percentage of

intercalated (*i.e.* amorphous) urea in the samples relative to total urea, $\%X_a$, was calculated as:

$$\%X_a = 100.\left(1 - \frac{100.\Delta H_m)}{W.\Delta H_0}\right) \qquad (1)$$

Where ΔH_m is the heat of fusion of urea in the kaolin-urea sample determined in the DSC thermogram, ΔH_0 is the heat of fusion of 100% crystalline urea determined from the DSC thermogram of urea and W is the mass percentage of urea in the kaolin-urea sample determined from TGA by the mass loss measured in the 135-400°C range. The heat of fusion relative to the fusion of urea (in J/g) was determined from the area under the melting endotherm of urea between 129 and 152°C in the DSC signal. The percentage of total urea, $\%U_{\mathrm{Tot}}$, in the sample calculated by removing the contribution of physisorbed water was determined from Eq. (2),

$$\%U_{\mathrm{Tot}} = 100.\frac{W}{(100-W_w)} \qquad (2)$$

Where W_{w} is the mass % of physisorbed water in the kaolin-urea sample determined from TGA by the mass loss measured in the 20-135°C range. The percentage of intercalated urea ($\%U_{\mathrm{Int}}$) in the kaolin-urea sample was determined using the following equation

$$\%U_{\mathrm{Int}} = \frac{X_a.\%U_{\mathrm{Tot}}}{100} \qquad (3)$$

Fig. 6 showed the amount of intercalated urea relative to total urea, $\%X_a$, and the amount of intercalated urea, $\%U_{\mathrm{Int}}$, in the kaolin-urea samples. After grinding for 2 h kaolin with 25 m% urea (KU-25), the intercalated urea content was 24.6 m% corresponding to 92 m% of the total urea. Three successive washing in isopropanol allowed the total elimination of external surface urea but this was accompanied by a partial deintercalation of urea, giving an intercalated urea content of 14.4 m%. The elimination of external urea required more extensive washing when kaolin was co-ground with 66 m% urea (KU-66). After seven

287 successive rinses with isopropanol, the intercalated urea content in KU-66 was 20.8 m%
288 corresponding to 79 m% of the total urea. Note that the content of intercalated urea is
289 certainly slightly overestimated because of loss of water between 135 and 400°C (gel water
290 formed during co-grinding and/or thermal dehydroxylation below 400°C during TGA ramp) .
291 XRD analyses of the samples were also carried out to determine the changes in the degree of
292 intercalation after isopropanol washes (Fig. 7). XRD patterns of KU-25 showed that the (001)
293 reflection collapsed partially to a *d*-value of 0.71 nm after the successive rinses with
294 isopropanol. This agrees with the DSC/TGA results that showed a significant deintercalation
295 of urea after isopropanol washes. On the other hand, KU-66 exhibited no collapse to a *d*-
296 value of 0.71 nm after isopropanol washing. DSC/TGA results of KU-66 indicated that
297 intercalated urea reduces from 26.8 m% to 20.8 m%, before and after seven successive
298 washes. These results suggest that a small deintercalation of urea during isopropanol rinses
299 was not necessarily accompanied by the collapse of the kaolinite layer.
300 *3.3. FTIR analysis*
301 FTIR spectra of the original kaolin and the ground kaolin-urea (25 m%) mixtures were shown
302 in Fig. 8. KGa-1b had the characteristic OH stretching pattern with 3687, 3669, and 3651 cm^{-1}
303 bands attributed to the inner surface hydroxyl groups of the alumina surface. The surface –
304 OH groups were accessible for hydrogen bonding with the intercalated molecules. Their
305 intensity and location are thus usually sensitive to the intercalation of organic molecules.
306 Another characteristic band at 3620 cm^{-1} is attributed to the stretching of the inner hydroxyl
307 groups. The inner-OH are located within the kaolinite framework and rarely interact with
308 organic intercalates (Elbokl and Detellier, 2009). Upon grinding kaolin with 25 m% urea for
309 different times, the absorption bands at 3687, 3669, and 3651 cm^{-1} from inner-surface
310 hydroxyl groups decreased with grinding times while the band at 3619 cm^{-1} remained

311 unperturbed. The infrared spectrum of urea was characterized by two strong bands at 3428
312 and 3334 cm^{-1} assigned to the NH_2 stretching vibrations. The weak band at 3254 cm^{-1} is
313 assigned to a combination band of the symmetrical NH_2-deformation and the CO stretching
314 vibration (Keuleers et al., 1999). These bands were observed in the infrared spectra of the
315 as-ground samples showing the presence of external urea for these samples. However, they
316 disappeared completely after washing with isopropanol, indicating that the excess external
317 urea was totally removed during the isopropanol washing. This is identical to the DSC/TGA
318 results. New bands also appeared at 3500, 3410, and 3387 cm^{-1}. The position of these new
319 bands was similar to those previously reported (Letaief et al., 2006a; Zhang et al., 2017).
320 They were related to NH_2 groups of urea involved in hydrogen bonds with inner-surface
321 hydroxyls. The antisymmetric and symmetric NH_2 stretching vibrations of urea in urea-water
322 solutions were reported at 3488 and 3379 cm^{-1}, respectively (Keuleers et al., 1999). The
323 corresponding bands shifted to higher wavenumbers in the FTIR spectra of Kaol-U
324 intercalates, supporting the weak hydrogen bonds between occluded urea and kaolinite. The
325 amine group of urea can interact as an H-donor with the oxygens of the tetrahedral sheet
326 (NH_2…O-Si) and with the oxygens of the hydroxyl groups on the alumina surface. The broad
327 3500 cm^{-1} band contains the contribution of the NH antisymmetric stretching of intercalated
328 urea with alumina and siloxane sheets in different environments. The bands at 3410 and
329 3387 cm^{-1} were due to the corresponding NH symmetric stretching vibrations. In the
330 literature, it was postulated that the 3380 cm^{-1} band corresponded to NH_2 groups interacting
331 with the siloxane sheet (Ledoux and White, 1966). It was more recently reported using
332 molecular dynamics simulation that the interaction energy of urea with alumina surfaces
333 was greater than that with siloxane surfaces (Zhang et al., 2017). The assignment of each of
334 the two bands at 3410 and 3387 cm^{-1} to a specific interaction with the siloxane or alumina

sheet is thus rather speculative. Another difference in the NH stretching region was the appearance of a poorly resolved band around 3450 cm^{-1}. The intensity of this band increased with grinding time but it is strongly reduced after extensive isopropanol washing. Seifi et al., (2016) noted absorption in the same wavelength range for Kaol-U intercalates and assigned this band to NH groups of urea linked to kaolinite by hydrogen bonding. The FTIR spectrum of KGa-1b (KBr pellet) gave two bands at 3457 and 1635 cm^{-1} that are related to OH stretching and OH deformation of water, respectively (Madejová and Komadel, 2001). The infrared spectra of the ground kaolin-urea mixtures did not show a well-resolved band at 1635 cm^{-1} due to overlapping with the strong NH_2 deformation bands but the intensity of the absorption around 1635 cm^{-1} increased with grinding time and strongly decreased after isopropanol washing. Thus, the most likely explanation of the 3450 cm^{-1} band is that it corresponded to adsorbed water formed by mechanochemical dehydroxylation and which was largely removed during extensive isopropanol washing. In the infrared spectrum of urea, the bands at 1674, 1618, 1588 and 1460 cm^{-1} were assigned to δ_s (NH_2), δ_{as}(NH_2), ν(CO) and ν_{as}(CN) vibrations, respectively (Grdadolnik and Maréchal, 2002). As the symmetrical NH_2 deformation and CO stretching vibrations are strongly coupled, any further discussion concerning the shifts of the 1674 and 1588 cm^{-1} bands would be purely speculative. The CN stretching vibration was shifted from 1460 to 1466 cm^{-1} in the spectra of the 2 h-ground kaolin-urea mixtures. After elimination of external urea by isopropanol washing, the CN stretching vibration of the intercalated urea was shifted to 1474 cm^{-1}. The increase in wavenumber indicated interactions in intercalated urea that strengthen the C-N bond. It suggests the formation of charge-transfer complex in which the oxygen atom of CO acts as an electron donor and the hydrogen atom of NH_2 as an electron acceptor resulting in C-N bond having more double bond character. This positive shift of ν_{as}(CN) band was similar to

359 that found by Zhang et al. (2017) and it supports their conclusion that the C=O groups of
360 urea acted as H-acceptors for the hydroxyl groups on alumina surfaces while the amino
361 group of urea acted as H-donor with basal oxygens on siloxane surfaces and/or with the
362 oxygens of hydroxyl groups on alumina surfaces. The position of the CN stretching vibration
363 of the as-ground samples (no isopropanol washing) reflected the presence of intercalated
364 urea and of some external crystals of urea. The bands at 1000 , 1025 (Si-O-Si in plane
365 vibrations) and 1115 cm^{-1} (apical Si-O) seen in Fig. S2 are the typical SiO bands of kaolinite
366 (Horváth et al., 2010). The bands at 1000 and 1025 cm^{-1}remained constant in position in the
367 spectra of Kaol-U intercalates; however two shoulders appear at ~1040 and ~1122 cm^{-1} that
368 were both increasing in intensity with grinding time. Thus, the local environment of Si atoms
369 was changed upon the intercalation of urea. Similar band shifts in the υ(Si-O) region have
370 been reported for hydrazine intercalated kaolinite (Johnston et al., 2000). Another means of
371 evaluating the changes in the structure of kaolinite upon intercalation is the study of the
372 AlOH bending region between 850 and 960 cm^{-1}. Kaolinite had two bands at 938 and 910 cm^{-1}
373 that can be assigned to the bending vibrations of the inner-surface hydroxyl and inner
374 hydroxyl, respectively. On grinding kaolin with urea an additional absorption appeared at
375 902 cm^{-1}. The intensity of 902 cm^{-1} bands increased with grinding time. Due to the
376 concomitant decrease of the 938 cm^{-1} band with increasing grinding time, it seems
377 reasonable to assign the 902 cm^{-1} band to the hydroxyl deformation vibration of the inner
378 surface hydroxyls hydrogen bonded to the C=O of urea, as proposed by Makó et al. (2009).
379 The decreasing intensity of the band at 902 cm^{-1} following washing with isopropanol
380 suggested that urea was partially deintercalated from kaolinite by washing. This result is
381 consistent with the XRD observations.

382 *3.4. Structural characteristics of kaolinite after urea washing*

383 The morphological changes which took place in the Kaol-U complexes after water washing
384 treatment were studied by XRD, FTIR, and TGA. Fig 9a showed the first basal diffractions of
385 kaolinite and Kaol-U intercalates after water washing treatments. Upon water washing of
386 the original KGa-1b or KGa-1b after 1 h grinding, the non-expanded (001) diffraction at 0.71
387 nm remained unchanged. The washed Kaol-U intercalates showed a more interesting XRD
388 pattern with a broad (001) reflection indicating the formation of a hydrate phase with a
389 poorly resolved XRD reflection centered around 0.84 nm and an additional phase at a slightly
390 higher interlayer distance than the original kaolinite (mean 0.76 nm). The XRD pattern of the
391 non-expanded kaolinite was thus not restored after the removal of urea by water washing.
392 Various synthetic kaolinite hydrates were reported with d-values near 0.84 nm (Tunney and
393 Detellier, 1994; Gardolinski et al., 2000; Valášková et al., 2007). A 0.76 nm reflection
394 appeared when a potassium acetate complex of a Georgia kaolinite was washed with water
395 (Deeds et al., 1966). Residual unexpanded (d-value = 0.71 nm) kaolinite was observed for the
396 washed Kaol-U intercalate prepared with 25 m% urea, which is not surprising when we take
397 into account that the Kaol-U intercalate with 25 m% urea contains 6% of non-expanded
398 kaolinite. The intensity in the 0.84 nm reflection of the hydrate as relative to the intensity of
399 the 0.76 nm reflection was slightly higher for the intercalate prepared with the higher
400 amount of urea (66 m%). Compared to the Kaol-U intercalates prepared with 25 m% urea, a
401 more pronounced reduction of the 001 diffraction intensity was observed for the kaolinite
402 intercalated with 66 m% urea. This suggests that the exfoliation/delamination of kaolinite is
403 more efficient when a high concentration of urea is used in the preparation of the Kaol-U
404 intercalate, in agreement with previous studies (Tsunematsu and Tateyama, 1999; Valášková
405 et al., 2007). The results of the thermal analyses of the water-washed samples were given in
406 Fig. 9b. The complete disappearance of the DTG peaks related to urea decomposition

407 indicated that urea was almost totally removed by the water washing procedure. The TGA
408 curves showed a continuous mass loss in the temperature range of 20-300°C due to
409 dehydration (and possibly residual urea for the co-ground samples) while the second mass
410 loss step between 350 and 700°C was due to the elimination of structural water. It was
411 noticeable that the DTG curve of the washed KU-66 intercalated with 66 m% urea showed
412 two distinct peaks at 44 and 190°C related to dehydration which suggested two types of
413 water in kaolinite. The sample prepared with 25 m% urea lost water in an apparently
414 continuous mass loss between 20 and 300°C. The mass loss due to dehydration
415 corresponded to 4.8% for the sample prepared with 66 m% urea and 4.4% for the sample
416 prepared with 25 m% urea, giving a stoichiometry of $Al_2Si_2O_5(OH)_4(H_2O)_{0.72}$ and
417 $Al_2Si_2O_5(OH)_4(H_2O)_{0.66}$, respectively. The stoichiometry of the water molecules thus found
418 was in accordance with the stoichiometry reported for 0.84 nm kaolinite hydrates prepared
419 from other kaolinite intercalates (Costanzo et al., 1984). Table 1 showed the variations in the
420 DTG dehydroxylation peak temperature with the milling and post-treatment conditions.
421 With increased grinding time, the dehydroxylation temperatures shifted to lower values and
422 it may be noted that the shift was more pronounced when kaolin was co-ground with a large
423 fraction of urea. Further, it appeared that when the crushed samples were subjected to
424 washing with isopropanol or urea removal upon immersion in water, the thermal
425 dehydroxylation temperature increased significantly again, while remaining lower than the
426 dehydroxylation temperature of the original kaolinite. The effect of isopropanol washes on
427 the dehydroxylation temperature was more pronounced with kaolin co-ground with low
428 fraction of urea (25 m%). This, combined with the fact that the washes of Kaol-U intercalates
429 with isopropanol induced a higher degree of deintercalation with urea loading of 25 m%,
430 implies that the drop in the dehydroxylation temperature was partly linked to the

interactions established by intercalated urea. Urea is almost completely decomposed when thermal dehydroxylation of kaolinite occurs. Therefore, it is in fact the residues of the decomposition of urea which, by interacting with the kaolinite, would be at the origin of the drop in the dehydroxylation temperature. On the other hand, dry grinding or co-grinding produced an increased amount of disordered and amorphous kaolinite phase (Aglietti et al., 1986a, 1986b; Gonzalez Garcia et al., 1991; Suraj et al., 1997; Sánchez-Soto et al., 2000; Frost et al., 2001b; Pardo et al., 2009; Vdović et al., 2010). The effect of the irreversible structural changes induced by grinding can be illustrated by observing the thermal behavior of the ground samples after the removal of urea by repeated washing with water. Compared to the original kaolinite, after co-grinding kaolin with 66 m% urea for 1 h and subsequent removal of urea by immersion in water, the dehydroxylation temperature showed a decrease of around 25°C. On the contrary, when kaolin was co-ground with 25 m% urea, there was a marginal decrease in the dehydroxylation temperature (~7°C after 2 h co-grinding). The decrease in dehydroxylation temperatures observed in this study appeared to be lower than that reported in a previous study about the Kaol-U complex obtained by mechanochemical intercalation (Makó et al., 2013). This confirmed that ball milling was performed under relatively mild conditions that did not result in a strong disorder of kaolinite. The remaining structural water after grinding kaolin or co-grinding kaolin with solid urea and subsequent washing of urea with water can be related to the relative mass losses in the range 400-800°C (Makó et al., 2009, 2013; Hamzaoui et al., 2015) (the amount of dehydroxylation water of the unground kaolin was considered to be 100% (Makó et al., 2009)). After 1 h of grinding, the relative mass loss of KGa-1b was 93%. After the kaolin was co-ground with 66 m% urea for 1/4 h and 1 h, the relative mass losses of dehydroxylation were 97% and 93%, respectively. After 1/4, 1 and 2 h co-grinding kaolin with 25 m% urea,

455 the relative mass losses of dehydroxylation were 100%, 95%, and 92%, respectively. These
456 results indicated that amorphization increased with the grinding time, with only a minor
457 effect of the urea content on the amorphization rate. On the other hand, the above values
458 showed that the ball milling conditions used in the present study led to minor amorphization
459 of kaolinite (after grinding or co-grinding with urea), notably comparing with other milling
460 conditions reported in previous studies (Makó et al., 2009, 2013). These findings are
461 consistent with the former XRD and SEM observations. The infrared spectra of the not-
462 ground kaolin and kaolin ground for 1 h after water washing were nearly identical to the
463 infrared spectrum of the original kaolin (Fig. 9c). The infrared spectra of the Kaol-U
464 intercalates after water washing showed a OH stretching band at 3545 cm^{-1} and a water
465 deformation band at 1652 cm^{-1} which support the formation of a kaolinite hydrate. These
466 spectral features were in good accord with those observed in the infrared spectra of the 0.84
467 nm hydrate prepared by washing with water an ethylene glycol intercalated kaolinite
468 (Tunney and Detellier, 1994). Additional changes were observed in the inner -OH band at
469 3619 cm^{-1} which was broader with the appearance of two shoulders at 3627 and 3609 cm^{-1}.
470 The shoulder at 3609 cm^{-1} can be interpreted as a red-shift of the 3619 cm^{-1} inner OH band.
471 The perturbance of the inner hydroxyls, as a red-shift, had been observed previously in other
472 0.84 nm hydrates and it supported the partial keying of water into the siloxane ditrigonal
473 cavity (Costanzo and Giese, 1990; Tunney and Detellier, 1994).

474 **4. Conclusion**

475 A summary of the advantages and limitations of the described mechanochemical
476 intercalation method can be given as follows. On the one hand, when kaolin is co-ground
477 with excess urea, a well-ordered complex is formed after a short grinding time but repeated
478 isopropanol washing is needed to remove excess urea. On the other hand, co-grinding

carried out with a lower amount of urea (close to the maximum urea content in the Kaol-U complex) promotes amorphization of kaolinite and requires long grinding times but no need for additional treatment. Complete intercalation of urea was achieved with very little amorphization of the kaolinite by grinding kaolin Kga1b with a small excess of urea (66 m%) in a ball mill for a short time (1/4 h). It was proposed that these results could be related to the specific grinding conditions used in this study: milling device, the jar and ball materials, and the use of a slight excess of urea relative to kaolinite. The Kaol-U intercalates prepared in this work will be used for the preparation of controlled-release fertilizer formulations through encapsulation with hydrogels to provide a humid- and nutrient-stable environment for plant growth.

Acknowledgements

This work was supported by the ANR through FCT in the framework of the ERA-NET project ProWsper - WaterJPI/0006/2016. The authors wish to thank C Chassigneux for performing the XRD measurements.

Notes

The authors declare no competing financial interest.

References

Aglietti, E.F., Porto Lopez, J.M., Pereira, E., 1986a. Mechanochemical effects in kaolinite grinding. II. Structural aspects. Int. J. Miner. Process. 16, 135–146. https://doi.org/10.1016/0301-7516(86)90080-3

Aglietti, E.F., Porto Lopez, J.M., Pereira, E., 1986b. Mechanochemical effects in kaolinite grinding. I. Textural and physicochemical aspects. Int. J. Miner. Process. 16, 125–133. https://doi.org/10.1016/0301-7516(86)90079-7

Cheng, H., Liu, Q., Xu, P., Hao, R., 2018. A comparison of molecular structure and de-intercalation kinetics of kaolinite/quaternary ammonium salt and alkylamine intercalation compounds. J. Solid State Chem. 268, 36–44. https://doi.org/10.1016/j.jssc.2018.08.009

Costanzo, P.M., Giese, R.F., 1990. Ordered and Disordered Organic Intercalates of 8.4-Å, Synthetically Hydrated Kaolinite. Clays Clay Miner. 38, 160–170. https://doi.org/10.1346/CCMN.1990.0380207

Costanzo, P.M., Giese, R.F., Lipsicas, M., 1984. Static and Dynamic Structure of Water in Hydrated Kaolinites. I. The Static Structure. Clays Clay Miner. 32, 419–428. https://doi.org/10.1346/CCMN.1984.0320511

Deeds, C., Van Olphen, H., Bradley, W., 1966. Intercalation and interlayer hydration of minerals of the kaolinite group. Proc. Int. Clay Conf. 183–199.

Elbokl, T.A., Detellier, C., 2009. Kaolinite–poly(methacrylamide) intercalated nanocomposite via in situ polymerization. Can. J. Chem. 87, 272–279. https://doi.org/10.1139/v08-142

Franco, F., Pérez-Maqueda, L.A., Pérez-Rodríguez, J.L., 2004. The effect of ultrasound on the particle size and structural disorder of a well-ordered kaolinite. J. Colloid Interface Sci. 274, 107–117. https://doi.org/10.1016/j.jcis.2003.12.003

Frost, R.L., Horváth, E., Makó, É., Kristóf, J., 2004. Modification of low- and high-defect kaolinite surfaces: implications for kaolinite mineral processing. J. Colloid Interface Sci. 270, 337–346. https://doi.org/10.1016/j.jcis.2003.10.034

Frost, R.L., Horváth, E., Makó, É., Kristóf, J., Rédey, Á., 2003. Slow transformation of mechanically dehydroxylated kaolinite to kaolinite—an aged mechanochemically activated formamide-intercalated kaolinite study. Thermochim. Acta 408, 103–113. https://doi.org/10.1016/S0040-6031(03)00316-2

Frost, R.L., Kristof, J., Rintoul, L., Kloprogge, J.T., 2000. Raman spectroscopy of urea and urea-intercalated kaolinites at 77 K. Spectrochim. Acta. A. Mol. Biomol. Spectrosc. 56, 1681–1691. https://doi.org/10.1016/S1386-1425(00)00223-7

Frost, R.L., Makó, É., Kristóf, J., Horváth, E., Kloprogge, J.T., 2001a. Modification of Kaolinite Surfaces by Mechanochemical Treatment. Langmuir 17, 4731–4738. https://doi.org/10.1021/la001453k

Frost, R.L., Makó, É., Kristóf, J., Horváth, E., Kloprogge, J.T., 2001b. Mechanochemical Treatment of Kaolinite. J. Colloid Interface Sci. 239, 458–466. https://doi.org/10.1006/jcis.2001.7591

Frost, R.L., Thu Ha, T., Kristof, J., 1997a. FT-Raman spectroscopy of the lattice region of kaolinite and its intercalates. Vib. Spectrosc. 13, 175–186. https://doi.org/10.1016/S0924-2031(96)00049-5

Frost, R.L., Tran, T.H., Kristof, J., 1997b. The structure of an intercalated ordered kaolinite; a Raman microscopy study. Clay Miner. 32, 587–596.

Gardolinski, J.E., Carrera, L.C.M., Cantão, M.P., Wypych, F., 2000. Layered polymer-kaolinite nanocomposites. J. Mater. Sci. 35, 3113–3119. https://doi.org/10.1023/A:1004820003253

Gardolinski, J.E.F.C., Lagaly, G., 2005a. Grafted organic derivatives of kaolinite: II. Intercalation of primary n-alkylamines and delamination. Clay Miner. 40, 547–556. https://doi.org/10.1180/0009855054040191

Gardolinski, J.E.F.C., Lagaly, G., 2005b. Grafted organic derivatives of kaolinite: I. Synthesis, chemical and rheological characterization. Clay Miner. 40, 537–546. https://doi.org/10.1180/0009855054040190

Gonzalez Garcia, F., Ruiz Abrio, M.T., Gonzalez Rodriguez, M., 1991. Effects of dry grinding on two kaolins of different degrees of crystallinity. Clay Miner. 26, 549–565.

553 Grdadolnik, J., Maréchal, Y., 2002. Urea and urea–water solutions—an infrared study. J. Mol.
554 Struct. 615, 177–189. https://doi.org/10.1016/S0022-2860(02)00214-4
555 Hamzaoui, R., Muslim, F., Guessasma, S., Bennabi, A., Guillin, J., 2015. Structural and thermal
556 behavior of proclay kaolinite using high energy ball milling process. Powder Technol.
557 271, 228–237. https://doi.org/10.1016/j.powtec.2014.11.018
558 Hinckley, D.N., 1962. Variability in "crystallinity" Values among the Kaolin Deposits of the
559 Coastal Plain of Georgia and South Carolina. Clays Clay Miner. 11, 229–235.
560 https://doi.org/10.1346/CCMN.1962.0110122
561 Horváth, E., Frost, R.L., Makó, É., Kristóf, J., Cseh, T., 2003. Thermal treatment of
562 mechanochemically activated kaolinite. Thermochim. Acta 404, 227–234.
563 https://doi.org/10.1016/S0040-6031(03)00184-9
564 Horváth, E., Kristóf, J., Frost, R.L., 2010. Vibrational Spectroscopy of Intercalated Kaolinites.
565 Part I. Appl. Spectrosc. Rev. 45, 130–147.
566 https://doi.org/10.1080/05704920903435862
567 House, K.A., House, J.E., 2017. Thermodynamics of dissolution of urea in water, alcohols, and
568 their mixtures. J. Mol. Liq. 242, 428–432.
569 https://doi.org/10.1016/j.molliq.2017.07.020
570 Johnston, C.T., Bish, D.L., Eckert, J., Brown, L.A., 2000. Infrared and Inelastic Neutron
571 Scattering Study of the 1.03- and 0.95-nm Kaolinite−Hydrazine Intercalation
572 Complexes. J. Phys. Chem. B 104, 8080–8088. https://doi.org/10.1021/jp001075s
573 Keuleers, R., Desseyn, H.O., Rousseau, B., Van Alsenoy, C., 1999. Vibrational Analysis of Urea.
574 J. Phys. Chem. A 103, 4621–4630. https://doi.org/10.1021/jp984180z
575 Kristóf, J., Frost, R., Horváth, E., Kocsis, L., Inczédy, J., 1998. Thermoanalytical Investigations
576 on Intercalated Kaolinites. J. Therm. Anal. Calorim. 53, 467–475.
577 https://doi.org/10.1023/a:1010189324654
578 Ledoux, R.L., White, J.L., 1966. Infrared studies of hydrogen bonding interaction between
579 kaolinite surfaces and intercalated potassium acetate, hydrazine, formamide, and
580 urea. J. Colloid Interface Sci. 21, 127–152. https://doi.org/10.1016/0095-
581 8522(66)90029-8
582 Letaief, S., Detellier, C., 2009. Clay−Polymer Nanocomposite Material from the Delamination
583 of Kaolinite in the Presence of Sodium Polyacrylate. Langmuir 25, 10975–10979.
584 https://doi.org/10.1021/la901196f
585 Letaief, S., Elbokl, T.A., Detellier, C., 2006a. Reactivity of ionic liquids with kaolinite: Melt
586 intersalation of ethyl pyridinium chloride in an urea-kaolinite pre-intercalate. J.
587 Colloid Interface Sci. 302, 254–258. https://doi.org/10.1016/j.jcis.2006.06.008
588 Letaief, S., Martín-Luengo, M.A., Aranda, P., Ruiz-Hitzky, E., 2006b. A Colloidal Route for
589 Delamination of Layered Solids: Novel Porous-Clay Nanocomposites. Adv. Funct.
590 Mater. 16, 401–409. https://doi.org//10.1002/adfm.200500190
591 Liu, Q., Zhang, S., Cheng, H., Wang, D., Li, X., Hou, X., Frost, R.L., 2014. Thermal behavior of
592 kaolinite–urea intercalation complex and molecular dynamics simulation for urea
593 molecule orientation. J. Therm. Anal. Calorim. 117, 189–196.
594 https://doi.org/10.1007/s10973-014-3646-1
595 Madejová, J., Komadel, P., 2001. Baseline studies of the clay minerals society source clays:
596 infrared methods. Clays Clay Miner. 49, 410–432.
597 Makó, É., Kovács, A., Antal, V., Kristóf, T., 2017. One-pot exfoliation of kaolinite by
598 solvothermal cointercalation. Appl. Clay Sci. 146, 131–139.
599 https://doi.org/10.1016/j.clay.2017.05.042

Makó, É., Kovács, A., Ható, Z., Kristóf, T., 2015. Simulation assisted characterization of kaolinite–methanol intercalation complexes synthesized using cost-efficient homogenization method. Appl. Surf. Sci. 357, 626–634. https://doi.org/10.1016/j.apsusc.2015.09.081

Makó, É., Kovács, A., Katona, R., Kristóf, T., 2016. Characterization of kaolinite-cetyltrimethylammonium chloride intercalation complex synthesized through eco-friend kaolinite-urea pre-intercalation complex. Colloids Surf. Physicochem. Eng. Asp. 508, 265–273. https://doi.org/10.1016/j.colsurfa.2016.08.035

Makó, É., Kovács, A., Kristóf, T., 2019. Influencing parameters of direct homogenization intercalation of kaolinite with urea, dimethyl sulfoxide, formamide, and N-methylformamide. Appl. Clay Sci. 182, 105287. https://doi.org/10.1016/j.clay.2019.105287

Makó, É., Kristóf, J., Horváth, E., Vágvölgyi, V., 2013. Mechanochemical intercalation of low reactivity kaolinite. Appl. Clay Sci. 83–84, 24–31. https://doi.org/10.1016/j.clay.2013.08.002

Makó, É., Kristóf, J., Horváth, E., Vágvölgyi, V., 2009. Kaolinite–urea complexes obtained by mechanochemical and aqueous suspension techniques—A comparative study. J. Colloid Interface Sci. 330, 367–373. https://doi.org/10.1016/j.jcis.2008.10.054

Miller, J.G., Oulton, T.D., 1970. Prototropy in Kaolinite during Percussive Grinding. Clays Clay Miner. 18, 313–323. https://doi.org/10.1346/CCMN.1970.0180603

Ondruška, J., Csáki, Š., Trnovcová, V., Štubňa, I., Lukáč, F., Pokorný, J., Vozár, L., Dobroň, P., 2018. Influence of mechanical activation on DC conductivity of kaolin. Appl. Clay Sci. 154, 36–42. https://doi.org/10.1016/j.clay.2017.12.038

Pardo, P., Bastida, J., Serrano, F.J., Ibáñez, R., Kojdecki, M.A., 2009. X-Ray Diffraction Line-Broadening Study on Two Vibrating, Dry-Milling Procedures in Kaolinites. Clays Clay Miner. 57, 25–34. https://doi.org/10.1346/CCMN.2009.0570102

Pruett, R.J., Webb, H.L., 1993. Sampling and Analysis of KGa-1B Well-Crystallized Kaolin Source Clay. Clays Clay Miner. 41, 514–519.

Rutkai, G., Makó, É., Kristóf, T., 2009. Simulation and experimental study of intercalation of urea in kaolinite. J. Colloid Interface Sci. 334, 65–69. https://doi.org/10.1016/j.jcis.2009.03.022

Sánchez-Soto, P.J., Haro, M. del C.J. de, Pérez-Maqueda, L.A., Varona, I., Pérez-Rodríguez, J.L., 2000. Effects of Dry Grinding on the Structural Changes of Kaolinite Powders. J. Am. Ceram. Soc. 83, 1649–1657. https://doi.org/10.1111/j.1151-2916.2000.tb01444.x

Schaber, P.M., Colson, J., Higgins, S., Thielen, D., Anspach, B., Brauer, J., 2004. Thermal decomposition (pyrolysis) of urea in an open reaction vessel. Thermochim. Acta 424, 131–142. https://doi.org/10.1016/j.tca.2004.05.018

Seifi, S., Diatta-Dieme, M.T., Blanchart, P., Lecomte-Nana, G.L., Kobor, D., Petit, S., 2016. Kaolin intercalated by urea. Ceramic applications. Constr. Build. Mater. 113, 579–585. https://doi.org/10.1016/j.conbuildmat.2016.03.095

Štefanić, G., Musić, S., Gajović, A., 2007. A comparative study of the influence of milling media on the structural and microstructural changes in monoclinic ZrO2. J. Eur. Ceram. Soc., Refereed Reports IX Conference & Exhibition of the European Ceramic Society 27, 1001–1016. https://doi.org/10.1016/j.jeurceramsoc.2006.04.136

Suraj, G., Iyer, C.S.P., Rugmini, S., Lalithambika, M., 1997. The effect of micronization on kaolinites and their sorption behaviour. Appl. Clay Sci. 12, 111–130. https://doi.org/10.1016/S0169-1317(96)00044-0

Tsunematsu, K., Tateyama, H., 1999. Delamination of Urea-Kaolinite Complex by Using Intercalation Procedures. J. Am. Ceram. Soc. 82, 1589–1591. https://doi.org/10.1111/j.1151-2916.1999.tb01963.x

Tunney, J., Detellier, C., 1994. Preparation and Characterization of an 8.4 Å Hydrate of Kaolinite. Clays Clay Miner. 42, 473–476. https://doi.org/10.1346/CCMN.1994.0420414

Valášková, M., Barabaszová, K., Hundáková, M., Ritz, M., Plevová, E., 2011. Effects of brief milling and acid treatment on two ordered and disordered kaolinite structures. Appl. Clay Sci. 54, 70–76. https://doi.org/10.1016/j.clay.2011.07.014

Valášková, M., Rieder, M., Matějka, V., Čapková, P., Slíva, A., 2007. Exfoliation/delamination of kaolinite by low-temperature washing of kaolinite–urea intercalates. Appl. Clay Sci. 35, 108–118. https://doi.org/10.1016/j.clay.2006.07.001

Vdović, N., Jurina, I., Škapin, S.D., Sondi, I., 2010. The surface properties of clay minerals modified by intensive dry milling — revisited. Appl. Clay Sci. 48, 575–580. https://doi.org/10.1016/j.clay.2010.03.006

Yan, C., Chen, J., Zhang, C., Han, K., 2005. Kaolinite-urea intercalation composites. Am. Ceram. Soc. Bull.

Zhang, S., Liu, Q., Gao, F., Li, X., Liu, C., Li, H., Boyd, S.A., Johnston, C.T., Teppen, B.J., 2017. Mechanism Associated with Kaolinite Intercalation with Urea: Combination of Infrared Spectroscopy and Molecular Dynamics Simulation Studies. J. Phys. Chem. C 121, 402–409. https://doi.org/10.1021/acs.jpcc.6b10533

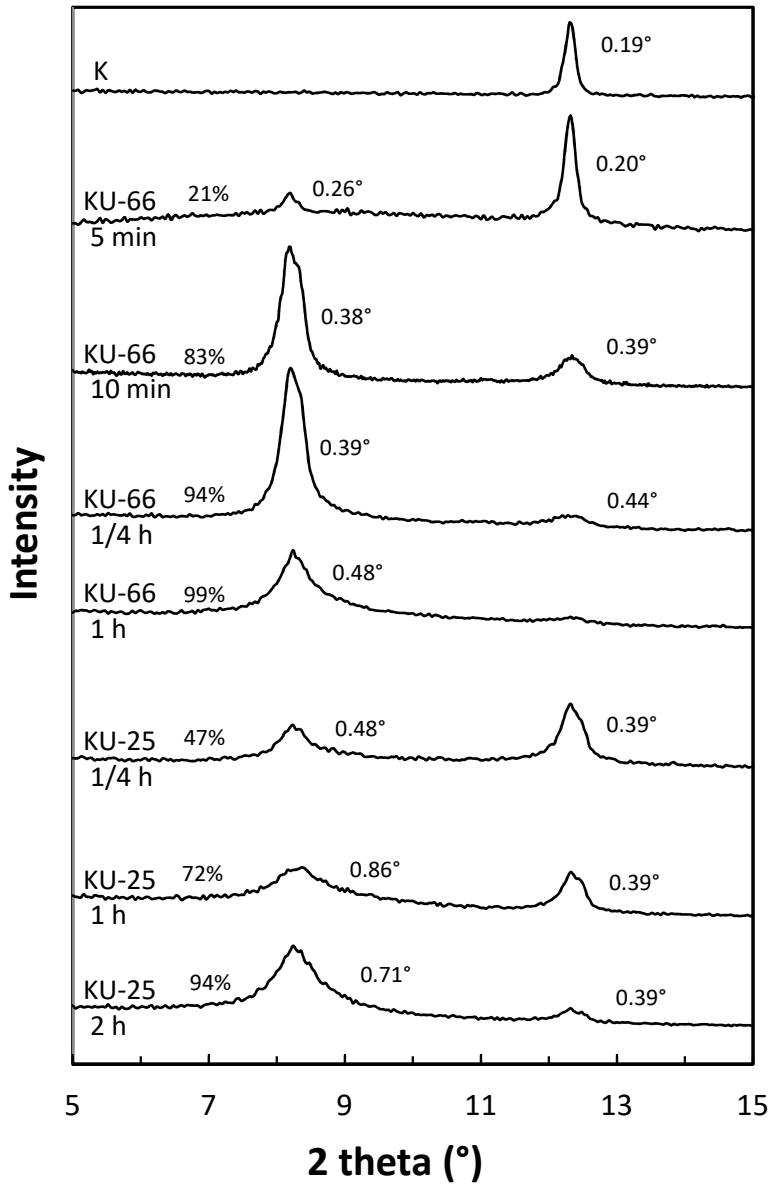

Fig. 1 X-ray diffraction patterns of the (001) reflection of original kaolin (KGa-1b) and kaolin mechanically ground together with 66 m% and (KU-66) and 25 m% (KU-25) solid urea (5 min-2h). The degree of intercalation, α (%) and the FWHM values (°) of the reflections of the expanded and non-expanded kaolinite are indicated. KU-25 and KU-66 were as ground samples.

680

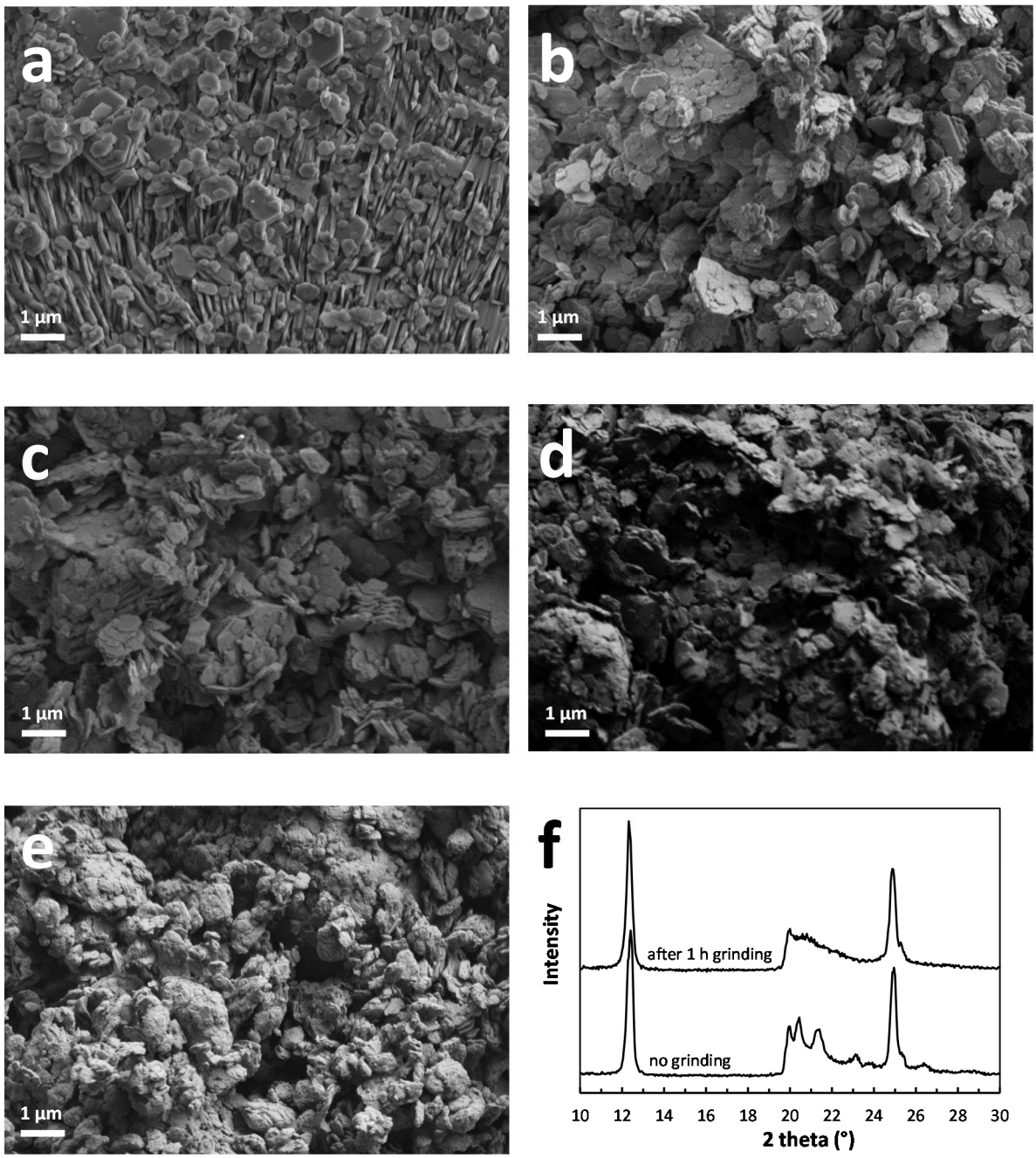

681

682

683 **Fig. 2.** SEM images showing the morphology of (a) original kaolin, (b) kaolin ground 1 h, (c)
684 kaolin ground 1/4 h with 66 m% urea, (d) kaolin ground 1 h with 66 m% urea, (e) kaolin
685 ground 2 h with 25 m% urea (samples c, d and e after repeated washing with isopropanol to
686 remove excess urea) and (f) XRD of kaolin before and after 1 h grinding.

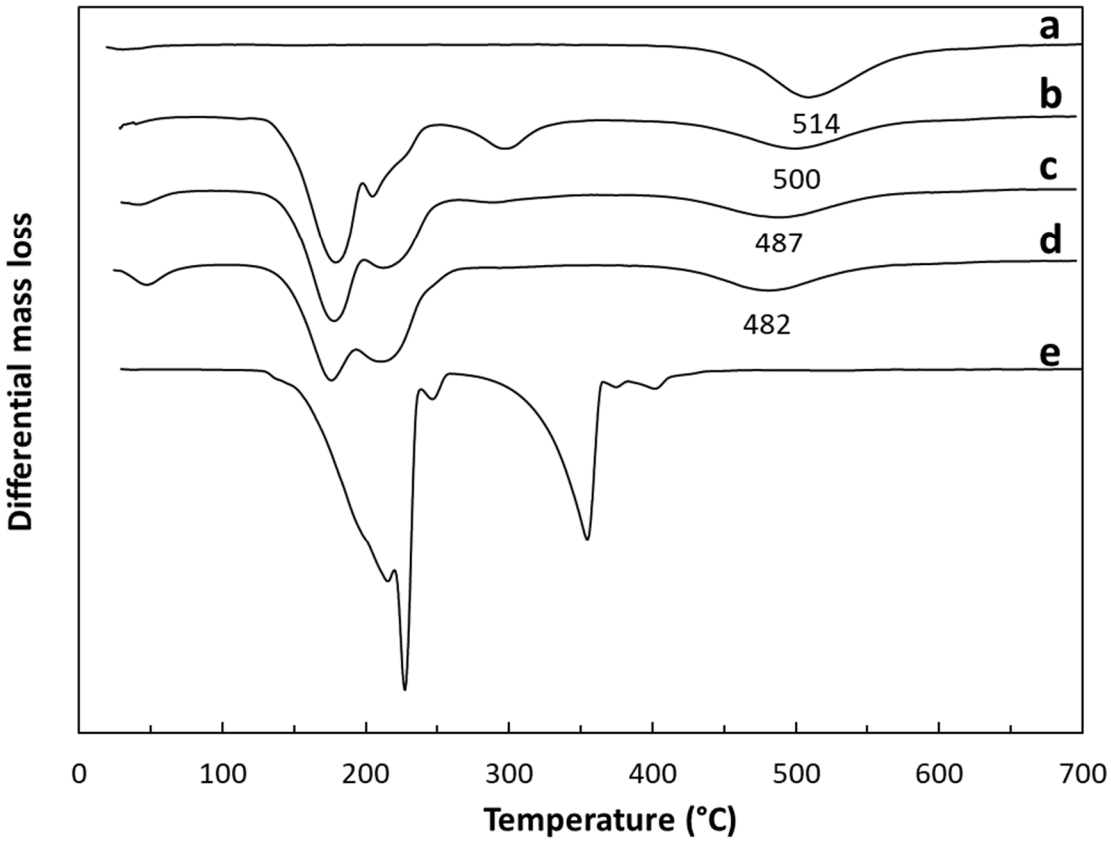

Fig. 3. Derivative thermogravimetric (DTG) curves of (a) original kaolin, (b) kaolin ground with 25 m% urea for 1/4 h (as ground), (c) kaolin ground with 25 m% urea for 1 h (as ground), (d) kaolin ground with 25 m% urea for 2 h (as ground) and (e) urea (the DTG peak temperatures of the thermal dehydroxylation of the kaolinite are indicated).

699

700

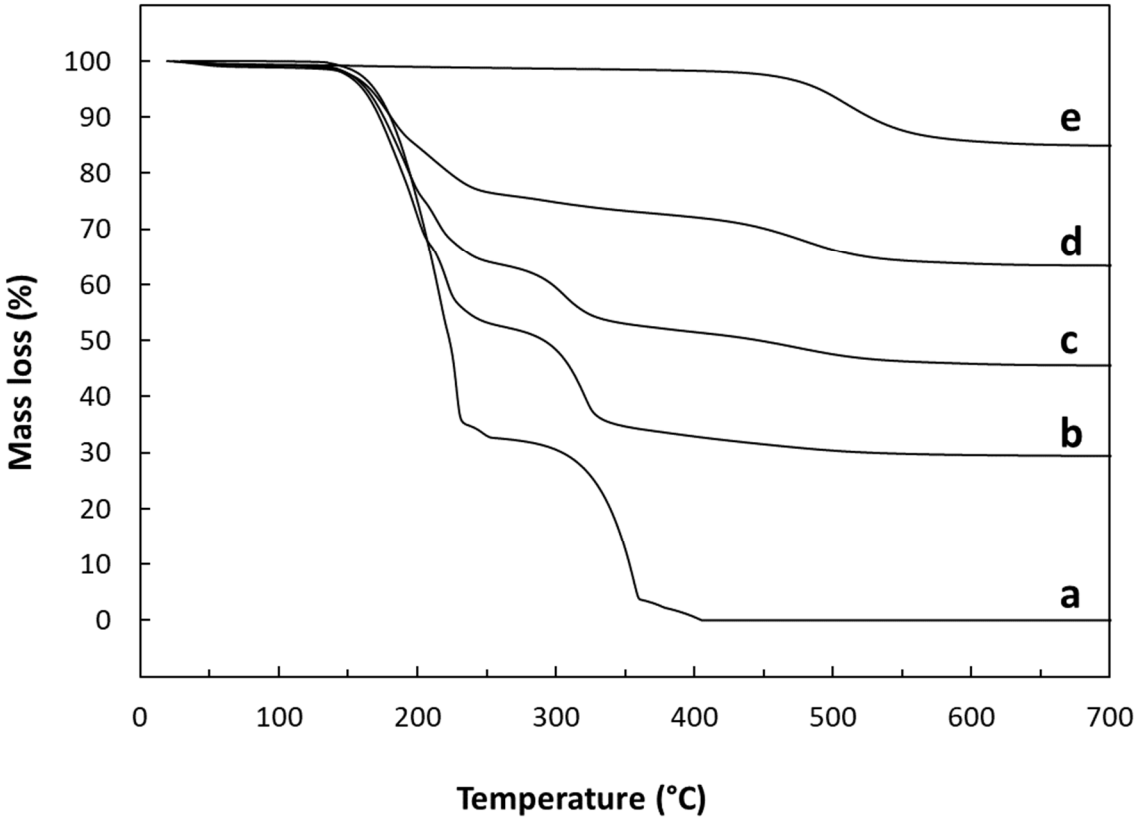

701

702

703 **Fig. 4.** Thermogravimetric analysis of (a) urea, (b) kaolin ground for 1 h with 66 m% urea, (c)
704 sample (b) washed three times with isopropanol, (d) sample (b) washed seven times with
705 isopropanol and (e) original kaolin.

706

707

708

709

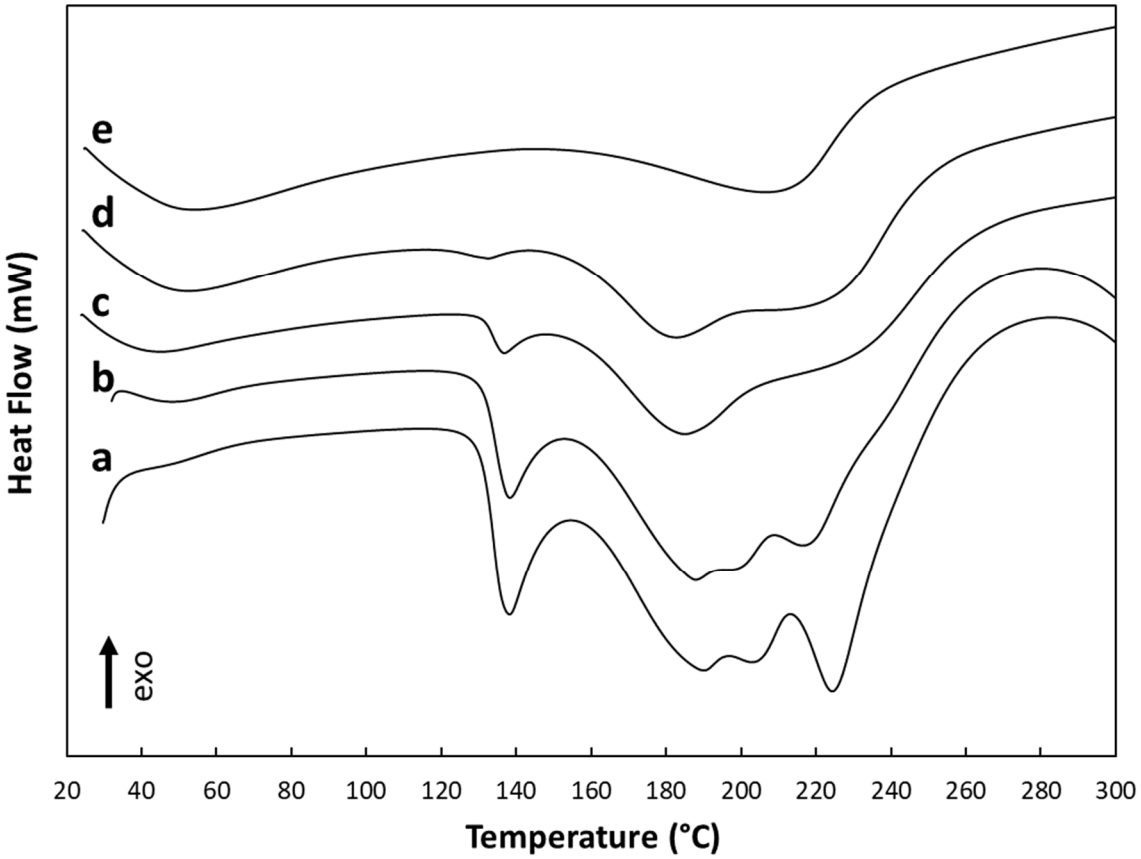

Fig. 5. DSC curves of (a) kaolin ground for 1 h with 66 m% urea (b) sample (a) washed three times with isopropanol, (c) sample (a) washed seven times with isopropanol, (d) kaolin ground for 2 h with 25 m% urea and (e) sample (d) washed three times with isopropanol.

720

721

722

723

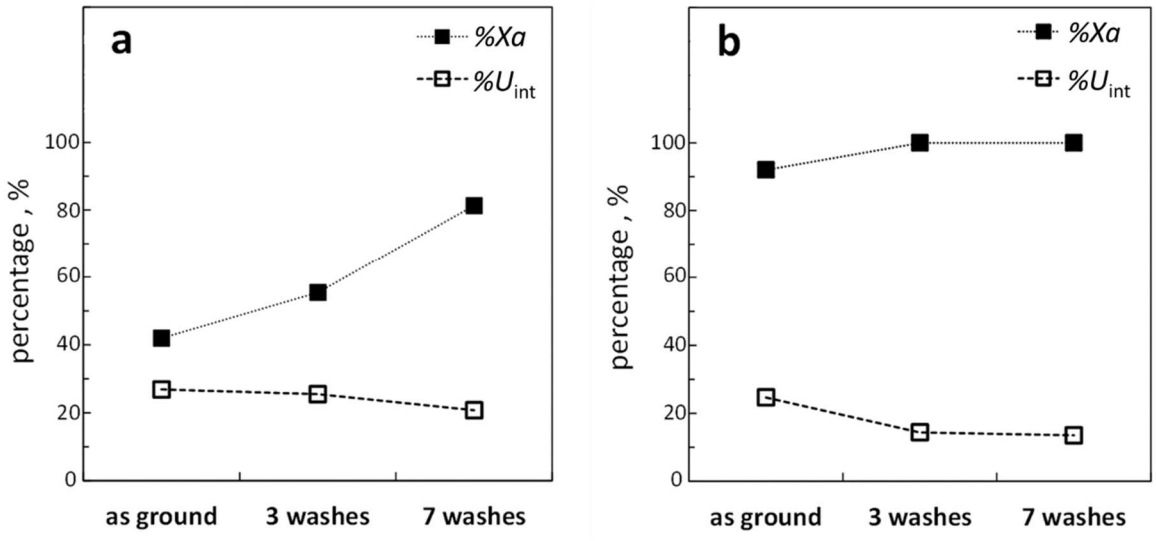

724

725 **Fig.6.** Effect of isopropanol washes on the amount of intercalated urea relative to total urea

726 (%X_a) or relative to the kaolin-urea content (%U_{Int}) for (a) kaolin ground with 66 m% urea for

727 1 h and (b) kaolin ground with 25 m% urea for 2 h. The error bars (the average deviation

728 from the mean of duplicate measurements) are smaller than the size of the symbols.

729

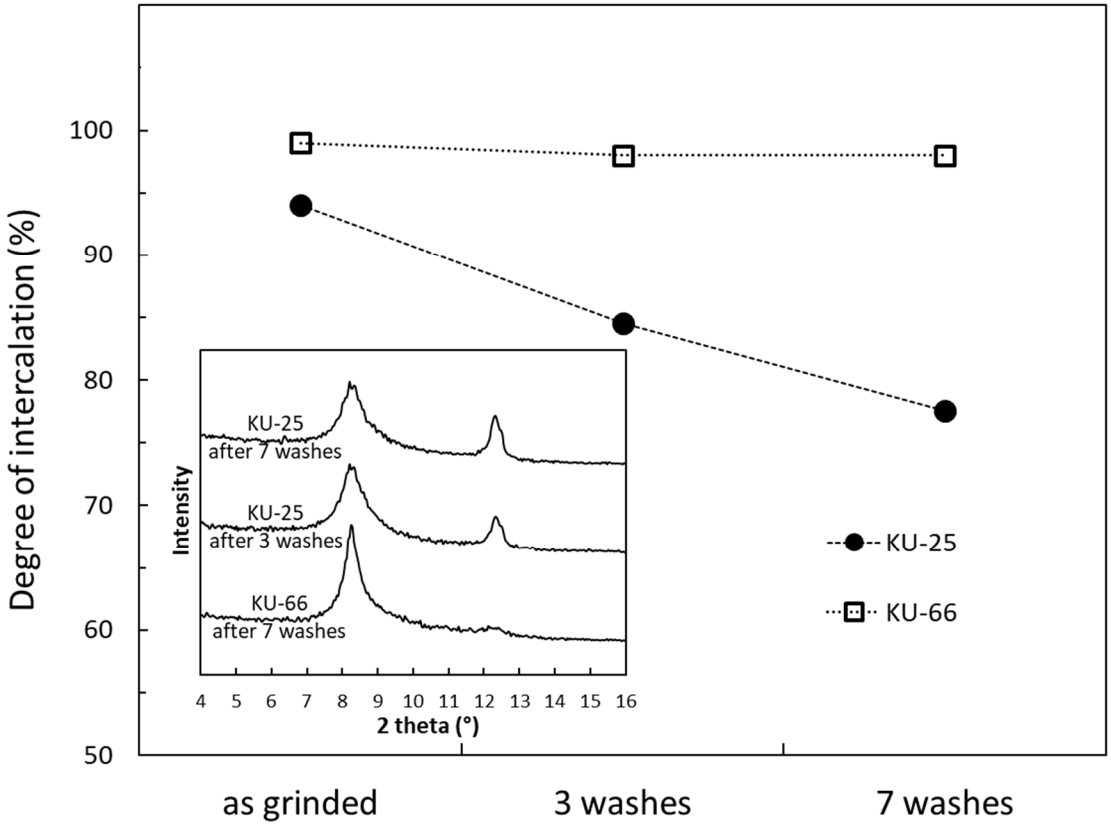

Fig. 7. Changes in the degree of intercalation calculated for the kaolin ground with 66 m% urea for 1 h (KU-66) and for kaolin ground with 25 m% urea for 2 h (KU-25) after isopropanol washes (XRD of KU-66 and KU-25 after washes with isopropanol are shown as inset). The error bars (the average deviation from the mean of duplicate measurements) are smaller than the size of the symbols.

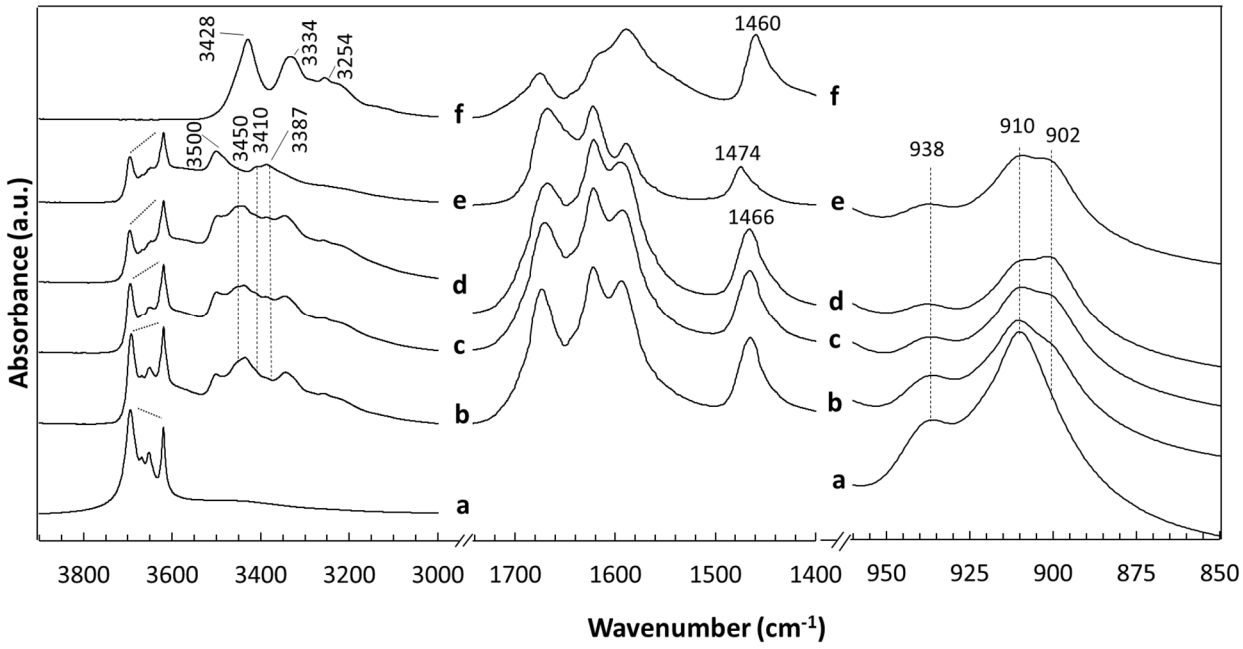

Fig. 8. Infrared spectra of (a) original kaolin, (b) the kaolin ground with 25 m% urea for (b) 1/4 h, (c) 1 h and (d) 2 h, (e) sample (d) washed three times with isopropanol and (f) urea.

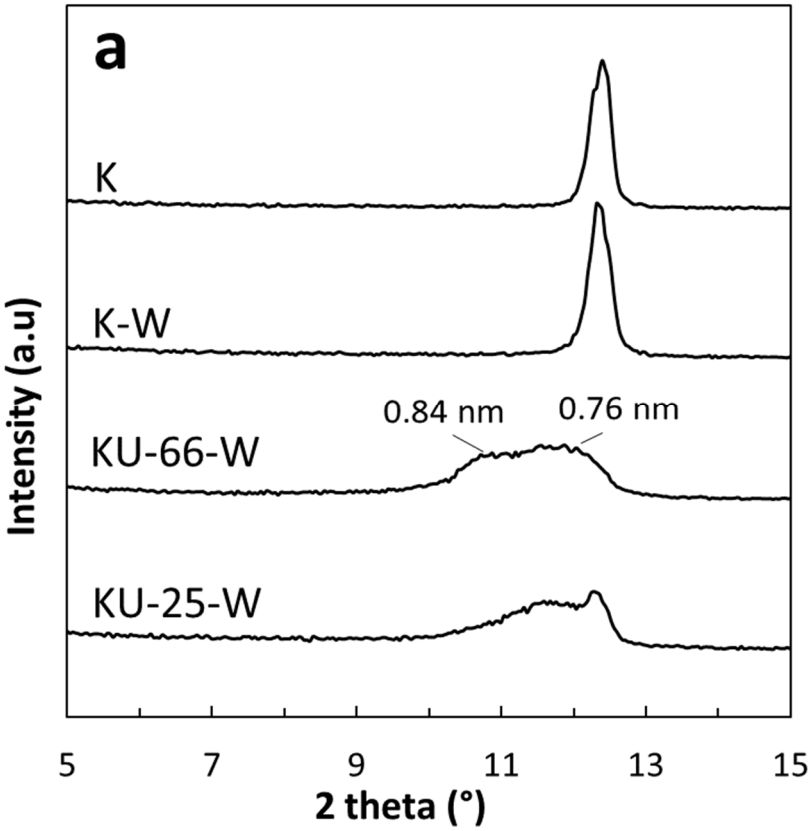
a
K
K-W
KU-66-W
KU-25-W
0.84 nm
0.76 nm
Intensity (a.u)
5
7
9
11
13
15
2 theta (°)

750

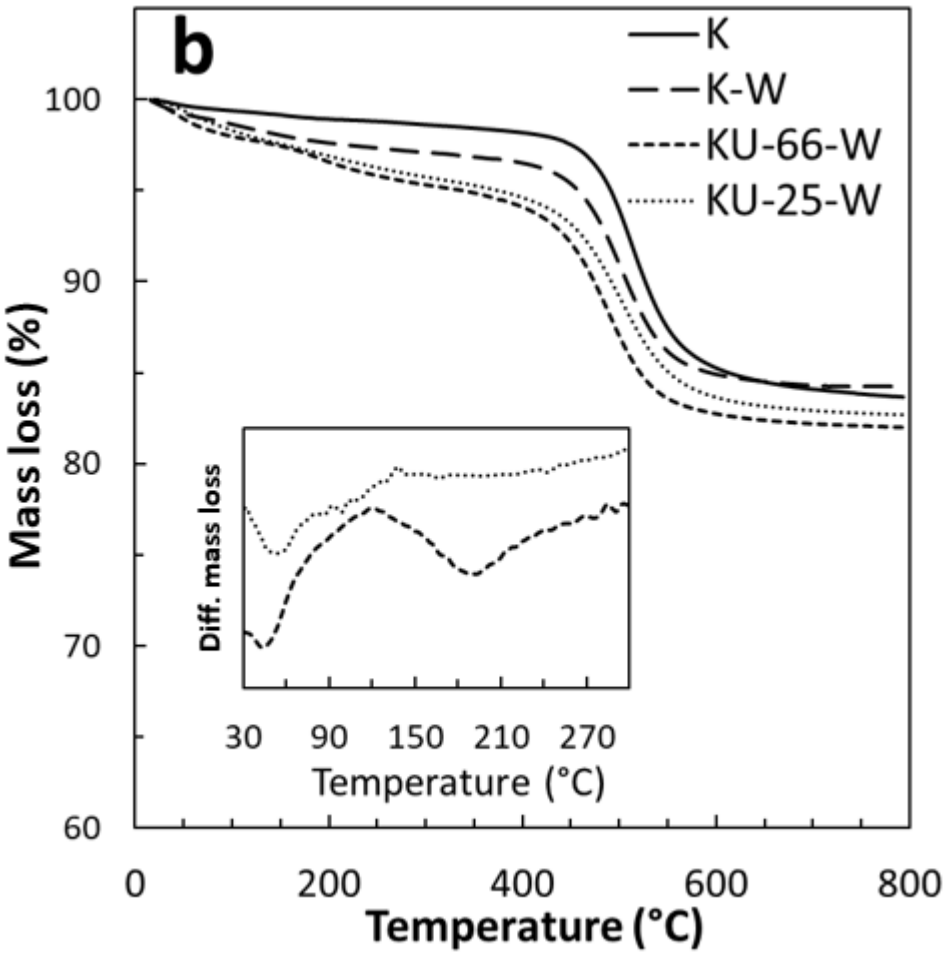
b
K
K-W
KU-66-W
KU-25-W
Mass loss (%)
100
90
80
70
60
0
200
400
600
800
Temperature (°C)
Diff. mass loss
30
90
150
210
270
Temperature (°C)

751

752

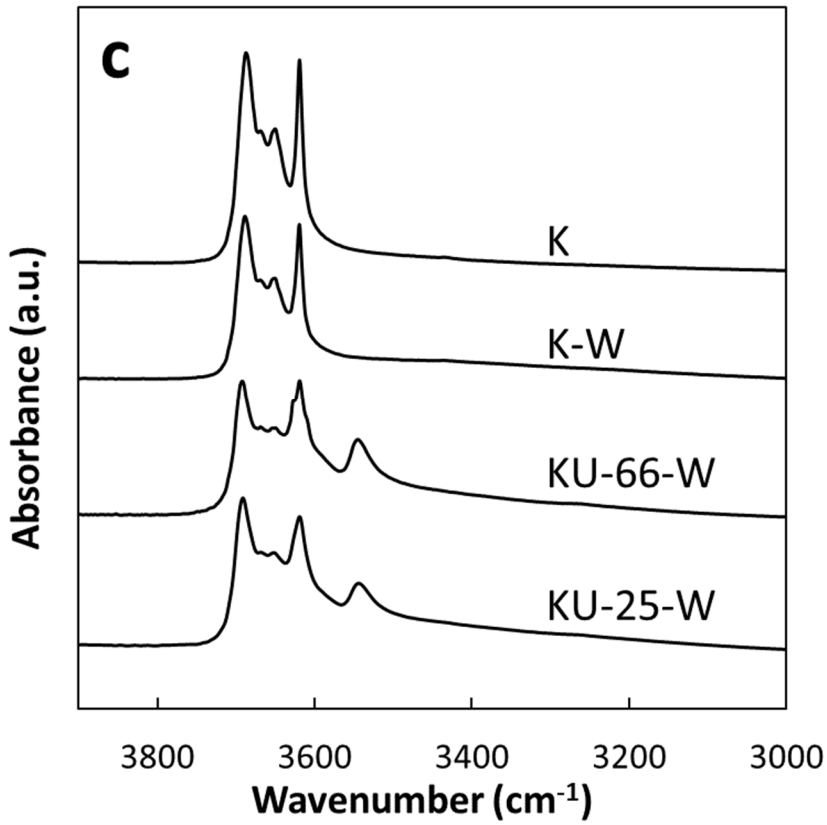

753

754

755 **Fig. 9.** (a) X-ray diffraction patterns of the (001) reflection, (b) thermogravimetric analysis
756 and (c) Infrared spectra in the range 3000-3900 cm^{-1} of original kaolin (K), kaolin ground for 1
757 h after water washing process (K-W), kaolin ground with 66 m% urea for 1 h after water
758 washing process (KU-66-W) and kaolin ground with 25 m% urea for 2 h after water washing
759 process (KU-25-W). The embedded graph in (b) shows the dehydration section of the DTG
760 curves of KU-25-W and KU-66-W.

761

762

763 **Table 1.**

764 Influence of milling conditions and washing steps on the DTG dehydroxylation peak

765 temperature (°C)

Milling conditions	Post-milling treatment			
	as ground	after three washes with isopropanol	after seven washes with isopropanol	after removal of urea with water
Kaolin no grinding	514			
Kaolin ground for 1 h	508			502
Kaolin ground for 1/4 h with 66 m% urea	486	491	498	502
Kaolin ground for 1 h with 66 m% urea	n.d.[a]	478	480	489
Kaolin ground for 1/4 h with 25 m% urea	500	504	506	513
Kaolin ground for 1 h with 25 m% urea	487	495	497	513
Kaolin ground for 2 h with 25 m% urea	482	488	489	507

766 [a] n.d. : not determined due to weak and broad signal